J Mater Sci (2011) 46:1890–1901
DOI 10.1007/s10853-010-5022-2

Studies on the friction and wear characteristics of rubber-based friction materials containing carbon and cellulose fibers

Akbar Shojaei · Mohammad Arjmand · Amir Saffar

Received: 10 August 2010 / Accepted: 20 October 2010 / Published online: 3 November 2010

Abstract The present study was an attempt to examine the effects of carbon and cellulose fibers on the tribological characteristics of rubber-based friction materials (RBFMs). A fiber free RBFM as a reference material and a series of fiber included RBFMs at different volume fractions were prepared by two-roll mill. The friction tests were performed at different sliding velocities and various drum temperatures. The mechanical properties and surface microstructure of friction specimens were also examined. It was revealed that the carbon fiber influences slightly the coefficient of friction (COF) of RBFM but it improves the wear resistance and the fade behavior considerably. It reduces the drum temperature as well. Cellulose fiber though offered high COF but it proved to be destructive from the fade behavior and wear rate point of view due to its weak thermal stability. It was found that the rubber-to-glass transition, which occurred at high sliding velocities, influences the COF, wear rate, and fade behavior of the RBFMs significantly for both fiber free and fiber-containing systems.

Introduction

The friction materials used in the brake system of any kind of vehicles should have stable and reliable coefficient of friction (COF) at wide range of braking load, vehicle speed, service temperature, humidity, and so on [1, 2]. These characteristics accompanied with high wear resistance, low noise, light weight, acceptable cost and easy processing make a friction material ideal for the brake system. The polymer-based composite materials have been known to be the best candidate to serve as friction materials in the brake system and to satisfy abovementioned requirements. The usefulness of polymer-based composite materials in the brake system is due to the presence of various ingredients in the compound including polymeric binder, fillers, friction modifiers, and fibrous reinforcements [3–5]. Such multi-component system takes the advantages of different materials which serve special functions in a single combined material.

Among many ingredients presently available for composite friction materials, polymeric binder plays a critical role on the tribological characteristics of the brake friction materials. The most widely used binder in the composite friction materials is the synthetic thermosetting resins, particularly phenolic resin [2, 6]. The high strength, good thermal resistance, and cost effectiveness of phenolic resin make this binder much suitable for wide range of applications such as automotive brake system. However, in the brake friction materials of heavy vehicles such as railroad locomotives and wagons, synthetic rubber may be used as the dominant polymeric binder inside which other ingredients are distributed uniformly [7, 8]. Due to the flexibility of the rubber materials, the corresponding rubber-based friction material (RBFM) is sufficiently soft and highly conformable. Typically, conformable composite friction materials have compression moduli below 500 MPa [9, 10]. The conformability is a key issue in the performance of the brake system of heavy duty vehicles such as railroad composite brake shoes. A brief history of the development of conformable friction material for the railroad vehicles has been addressed by Gibson [10]. It is believed that the conformable brake shoes reduce hot spots

A. Shojaei (✉) · M. Arjmand · A. Saffar
Department of Chemical and Petroleum Engineering,
Sharif University of Technology,
P. O. Box 11155-9465, Tehran, Iran
e-mail: akbar.shojaei@sharif.edu

and thermal stresses of the wheels (counterfaces) significantly [10]. This is possible through larger real contact area achievable for this kind of friction materials leading to the distribution of braking energy over the wheel more uniformly [9–11].

The phenolic resin-based composite friction materials have been extensively investigated. It has been shown that the type of phenolic resin, i.e., modified and unmodified ones, has crucial role on the frictional characteristics of the resin-based friction materials [2, 12–14] such as fade, i.e., loss of COF at elevated temperature, and recovery, i.e., the revival of COF after temporary exposure to braking-induced thermal elevation [12, 13, 15]. Incorporation of suitable ingredients with high thermal conductivity, good thermal stability, and acceptable mechanical properties has been known to be practical solution for improving frictional characteristics of the thermosetting binder. One of the essential ingredients, which can improve considerably the tribological characteristics of the resin-based friction materials, has been shown to be the short reinforcing fibers [4, 16–19]. However, the frictional characteristics of the RBFMs and the influence of short fibers on the friction and wear of this kind of friction materials have been rarely reported in the literature [9, 20, 21]. Recently, Shojaei and coworkers [22] observed that the COF and wear rate of RBFM undergo a steep change at higher sliding velocity which was attributed to the rubber-to-glass transition in this type of friction materials.

Various non-asbestos fibers, e.g., metallic, glass, ceramic, and organic fibers, have been widely employed in the friction materials [23–26]. Among the fibers currently used in the friction materials, carbon and cellulose fibers have attracted much attention due to their good performance and suitable processability. Carbon fibers show attractive characteristics such as great tolerance to high temperature and corrosive environment, high mechanical performance, good moisture resistance, and superior thermal conductivity [27, 28]. In addition, cellulose fiber indicates good reinforcing efficiency, low squeal, helpful resiliency, low cost as well as serving as processing aid [15, 29, 30].

The influence of carbon fiber and cellulose fiber on the frictional performance of composite friction materials has been reported in the literature. All of these studies have focused on the resin-based friction materials. Gopal et al. [19] stated that at high temperatures and high sliding velocities, friction material containing carbon fiber indicates less wear resistance and higher COF than glass fiber added composite but it shows lower specific wear rate at low speeds and low sliding temperatures over a wide range of applied loads. Satapathy and Bijwe [29] reported that composites holding carbon and cellulose fibers demonstrate the lowest and highest amount of COF, respectively, among all organic fiber added composites over various operating conditions. They [15] also asserted that carbon fiber improves the wear resistance and reduces the COF while cellulose fiber increases the COF but it shows detrimental effect on wear resistance of the composite. Contrarily, Griffith [31] noticed that the wear rate of friction materials for locomotive brake shoes is improved by incorporation of reinforcing fibers such as cellulose fiber.

The objective of the present work was to investigate the tribological characteristics of RBFM and the influence of two different fibers including carbon and cellulose fibers on the performance of this kind of friction materials. In this study, a fiber free RBFM was selected as a reference material, called RM, and then carbon fiber and cellulose fiber were incorporated in the RM with varying volume fractions. Then the physico-mechanical properties and frictional characteristics of these composites were analyzed experimentally.

Experimental procedure

Materials and preparation of test specimens

Styrene butadiene rubber (SBR 1502) from BIPC (Bandar Imam Petrochemical Company, Iran) was used as the rubber binder. Phenolic resin (Novolac IP 502) from Rezitan Co. (Iran) was utilized to strengthen and stiffen the rubber binder. Mercaptobenzthiazyl disulfide (MBTS), zinc oxide, stearic acid, and sulfur were employed as the curing agents of SBR. Coal powder, iron powder, calcium carbonate, barite, and iron oxide (both magnetite and limonite) were used as filler in the friction materials. Carbon fiber (T-300) was supplied by Fajr Co. (Iran) and cellulose fiber was donated by Machinlent-e-Tehran Co. (Iran).

In this study, a RBFM without fiber was utilized as RM. Carbon fiber and cellulose fiber were incorporated into the RM at two different concentrations. Table 1 shows the composition of both fiber-filled composites and the RM in terms of volume fraction. The volume fraction of each component in the compounds was obtained based on the corresponding weight fraction and the densities of relevant component and the whole composite according to the procedure mentioned elsewhere [20]. The fibers were added in the composite in such a way that the volume fraction of polymer component was kept almost the same as RM. This was done in a way that the addition of fiber led to the reduction in volume fraction of all fillers proportional to their volume. This causes a slight difference in composition of fillers between the RM and fiber added composites. However, the polymer component, particularly the rubber component, still forms the dominant portion of the composition. The composites containing fibers of carbon and cellulose were denoted by CAR and CEL, respectively, followed by a number indicating the

Table 1 Composition of friction materials used in this study in terms of volume fraction

Composite	Polymer component[b] (vol.%)	Filler[c] (vol.%)	Fiber (vol.%)
RM[a]	0.53	0.47	0
Comp 1	0.53	0.395	0.075
Comp 2	0.53	0.32	0.15

[a] RM: friction material without any fiber; Comp 1: composite with 7.5 vol.% of fiber; Comp 2: composite with 15 vol.% fiber. The fiber in Comp 1 and Comp 2 can be either carbon or cellulose

[b] Polymer component includes SBR 1502 plus curing agent including sulfur, accelerator, zinc oxide, and stearic acid (45 vol.%) and phenolic resin (8 vol.%)

[c] Fillers include coal powder, calcium carbonate, iron powder, barite and iron oxide (both magnetite and limonite)

concentration of corresponding fibers in terms of volume percent. For instance, CAR 7.5% showed a RBFM filled with 7.5 vol.% carbon fiber.

All ingredients were mixed using a two-roll mill at the room temperature with a slight warming the compounds up due to the mixing cycle. Prior to mixing, the fillers were dried in an oven at 70 °C under vacuum for 24 h in order to remove the physically adsorbed and weakly chemically absorbed species. The test specimens were prepared by compression molding at 145 °C and 100 MPa for 40 min followed by post-curing at 150 °C for 5 h.

Friction and wear tests

Friction and wear tests were conducted on a chase type friction testing machine developed in our laboratory by Mahtablent Co. (Iran) according to SAE J661. Figure 1 shows the friction testing machine used in this study. The friction testing machine is fully computer controllable and involves data acquisition software. It consists of a cast iron drum with a nominal diameter of 300 mm, which is connected to a 7.5 kW three-phase AC motor. In order to control the drum temperature at a preset value, an electric heater and an air blower installed close to the drum are utilized. Drum temperature is measured using the K-type thermocouples mounted below the sliding surface of the drum. The drum rotation speed and the drum temperature can be adjusted using a PC-based software. The friction specimen includes a sample with the friction surface of 25 × 25 mm.

The friction test used in this study consisted of three sequential stages including (1) preliminary, (2) thermal, and (3) complementary stages. Test mode in the preliminary and the complementary stages was comprised of a 10 s drag followed with 10 s interval which was repeated 20 times consecutively. The thermal stage was instantly started after preliminary stage during which continuous braking was applied. As a matter of fact, the temperature of the drum increased in the course of thermal stage using the electric heater and friction-induced heat. This stage would be completed after predefined time, i.e., 10 min, or after arriving the drum temperature to a specified value, i.e., 350 °C, whichever was reached earlier. The ratio of friction force (measured by load cell having capacity of 100 kg_f, OBU-100, Bongshin loadcell Co., Ltd., Korea) to the normal load was given as the COF at each stage. The normal load used in this study was a fixed value of 45.4 kg_f. A typical friction curve showing all three stages is displayed in Fig. 2. During the friction tests, the COF and the drum temperature were recorded continuously. At least, 20 data points were recorded for each stage. Three different average friction coefficients are used to analyze the frictional behaviors. These are $\bar{\mu}$ (average COF for the whole testing cycle including preliminary, thermal, and complementary stages), $\bar{\mu}_P$ (average friction coefficients for the preliminary stage), and $\bar{\mu}_C$ (average friction coefficients for the complementary stage). Accordingly, friction coefficient recovery (μ-recovery) percent and μ-fade percent are defined as follows:

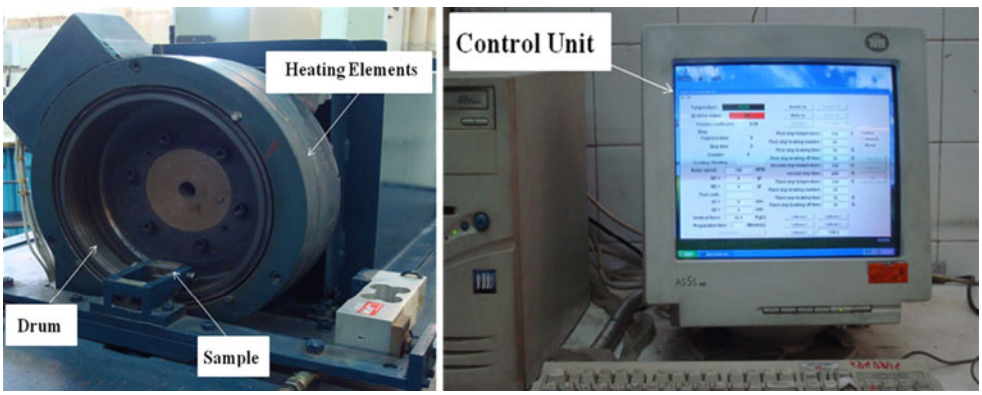

Fig. 1 Friction testing machine used in this study

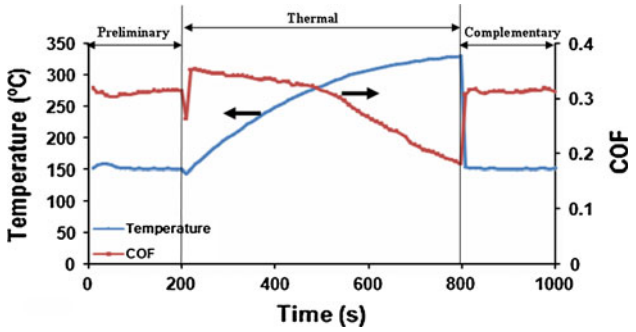

Fig. 2 Variation of drum temperature and COF during the friction test obtained from friction tester for a typical sample (CEL 7.5%, 700 rpm, temperature cycle 150–350–150 °C)

$$\mu\text{-recovery } (\%) = [\bar{\mu}_C/\bar{\mu}_P] \times 100 \quad (1)$$

$$\mu\text{-fade } (\%) = [(\bar{\mu}_P - \mu_f)/\bar{\mu}_P] \times 100, \quad (2)$$

where μ_f is the minimum friction coefficient in the thermal stage. The specific wear rate SW (cm^3/N m) was determined using the following relation

$$SW = \Delta m/\rho FL, \quad (3)$$

where Δm (g) is the cumulative weight loss after the completion of friction test, ρ (g/cm^3) is the density of the sample, F (N) is the average friction force, and L (m) is the sliding distance.

In this study, the friction tests for each composite were performed at sliding velocities of 300, 500, and 700 rpm each at 150 °C and also at temperatures 100, 150, and 200 °C all at 700 rpm. It should be pointed out that these temperatures were the drum temperature at preliminary and complementary stages, while the temperature during the thermal stage was allowed for increasing from the preset temperature at preliminary stage up to 350 °C. As a matter of fact each sample experienced a temperature cycle during a friction test. For instance, temperature cycle indicated by the designation of 150–350–150 °C showed the temperature at the three stages of the friction tests consecutively. Friction tests were repeated at least three times for a given composition at a specified braking condition to obtain repeatable data.

Characterizations

Hardness of the friction specimens was measured using a Rockwell hardness tester (HR-150A, Shengya Machine & Tools Co. Ltd., China) according to UIC 541-4 OR [32]. Accordingly, the surface hardness was expressed in terms of HRX, i.e., scale X with a steel ball indenter having 19 mm diameter [9, 32]. The density of the specimens was determined based on Archimedes' principle according to ASTM D792. The surface roughness values of the specimens before and after the friction tests were measured by a portable surface roughness apparatus (Mahr Federal Inc., Germany). The worn surface of the friction materials was examined using scanning electron microscopy (SEM, VEGA TS-5136 MM).

Results and discussion

Physical and mechanical properties

The physical properties of all friction materials are listed in Table 2. As it is evident, the carbon fiber leads to loss in the surface hardness. Contrarily, despite the inherent softness of cellulose fiber, it shows sensible positive influence on the surface hardness of the RBFMs. This behavior of cellulose fiber-containing composites may be attributed to better dispersion of the cellulose fiber and its better interaction with the binder. Such behavior can be explained by the fact that the cellulose fiber is natural organic-based polymer having many functional chemical groups [33] which more likely enable the cellulose fiber to interact with the binder efficiently.

Table 2 denotes that incorporation of carbon fiber and cellulose fiber results in a loss in the density of the composites slightly. As the density of carbon fiber is around 1.8 g/cm^3 [28], the reduction of density for carbon fiber added composites may be due to the void formation during the processing. However, the lower density of cellulose fiber added composites could be due to lower density of this fiber, i.e., 1 g/cm^3 [15].

Table 2 also demonstrates the surface roughness of all composites before and after friction tests at temperature cycle 150–350–150 °C and sliding speed 700 rpm. As it is evident, incorporation of fibers (both cellulose and carbon) into the RM enhances the surface roughness of the samples which may contribute to the plowing component of the friction [34, 35]. In addition, it is seen that the surface roughness of each composite increases upon friction test. However, the trend of variation of surface roughness for each fiber is different. Actually, carbon fiber added composites show a greater surface roughness after the friction test with respect to RM, while this behavior is different for

Table 2 Physical properties of composites friction materials

Properties	HRX	Density (g/cm^3)	Roughness (μm) (before wear)	Roughness (μm) (after wear)
RM	29	1.74	1.68	3
CAR 7.5%	21	1.67	1.75	3.96
CAR 15%	24	1.62	1.98	2.48
CEL 7.5%	36	1.61	1.85	2.64
CEL 15%	41	1.5	1.99	2.33

cellulose fiber added samples. This suggests that the wear mechanism is different for these two fiber added composites, showing the dominant role of fiber in the wear characteristics.

Friction and wear characteristics of RBFMs

Effect of sliding speed and temperature cycle on frictional behavior

Table 3 exhibits $\bar{\mu}$ and the μ-recover versus sliding velocity. As can be inferred, the influence of fibers on the $\bar{\mu}$ follows this order: CEL $\gg$ CAR $>$ RM. This indicates that the friction coefficient of RBFM increases with incorporation of both carbon fiber and cellulose fiber. However, the extent of enhancement with cellulose fiber is much higher. According to Table 3, $\bar{\mu}$ does not change sensibly with sliding velocity for the RM, i.e., rubber-based material without fiber; however, incorporation of fibers (except CELL 15%) increases slightly $\bar{\mu}$.

As it is seen in Table 3, the carbon fiber cannot enhance the $\bar{\mu}$ of RBFMs as much as the cellulose fiber. This can be possibly attributed to the competition of lubricating role of carbon fiber [34] and easier formation of transfer layer for CAR composites [1] with enhanced plowing component of friction force caused by the higher surface roughness (see Table 2 for surface roughness). Lubricating effect of carbon fiber can be ascribed to its multilayer microstructure, i.e., graphitic layers, which can slip over each other easily, leading to a lower amount of input stress to be registered as frictional output. In addition, the formation of transfer layer leads to weak polymer–polymer adhesion between transfer layer and friction surface [35], while the plowing mechanism tends to increase the COF.

As it is evident in Table 3, cellulose fiber added composites exhibit highest amount of $\bar{\mu}$ among all employed composites. This behavior can be partly attributed to the large amount of abrasive wear debris formed by the thermal- and shear-induced degradations of cellulose fiber [15, 34]. Thermal degradation of cellulose fiber occurs relatively at low temperature, i.e., 140–200 °C [15, 33, 36, 37]. Such wear debris have been known to act as third body abrasion agents and help to increasing COF [37–39]. The results show that the $\bar{\mu}$ of cellulose fiber added composites indicates a decreasing trend with sliding speed for highly loaded cellulose fiber composite. This can be possibly explained by higher friction-induced heat caused by higher friction coefficient of this material which may result in higher flash temperature at asperities and severe thermal degradation of cellulose fiber.

Table 3 $\bar{\mu}$ and μ-recovery versus sliding velocity at temperature cycle of 150–350–150 °C

Sliding velocity (rpm)	Material				
	RM	CAR 7.5%	CAR 15%	CELL 7.5%	CELL 15%
300 rpm					
$\bar{\mu}$	0.24	0.27	0.24	0.31	0.36
μ-Recovery (%)	92	97	89	92	91
500 rpm					
$\bar{\mu}$	0.24	0.28	0.25	0.32	0.34
μ-Recovery (%)	97	110	114	100	100
700 rpm					
$\bar{\mu}$	0.25	0.29	0.25	0.33	0.34
μ-Recovery (%)	102	117	115	108	107

Table 3 represents the μ-recovery of the composites at different sliding velocities tested at temperature cycle of 150–350–150 °C. Because of changes in morphology of the surface, formation of new materials and changes in frictional stability of the ingredients during thermal stage, COF in complementary stage is different from what recorded in preliminary stage. As it is inferred from Table 3, incorporation of fibers (both cellulose and carbon) increases the μ-recovery of the RBFM particularly at higher sliding velocities where higher frictional heat is supposed. However, the influence of carbon fiber on the μ-recovery is higher compared to the cellulose fiber. This can be attributed to the high thermal stability and high thermal conductivity of carbon fiber [40, 41] and the relevant composites which resist against thermal degradation and facilitate the heat transfer from the mating surface and consequently reduce the flash temperatures at the asperities.

The influence of the drum temperature on the $\bar{\mu}$ and the μ-recovery is presented in Table 4. As can be inferred, the $\bar{\mu}$ decreases with the drum temperature during the friction test. This can be ascribed to the loss in mechanical properties, leading to lower deformation energy, as well as weakened interfacial interaction at the contacting surface [34, 35]. In addition, it is deduced that the μ-recovery is improved by the incorporation of both carbon and cellulose fibers at different drum temperatures. This exhibits the critical influence of the fibers in the recovery of COF in RBFMs. Much higher recovery of CEL 15% can be attributable to the higher extent of degradation of cellulose fiber at higher temperature which leads to the production of high amount of wear debris. The wear debris can then serve as COF enhancing agents in the complementary stage.

Thermal and fade behaviors

Fade indicates the loss in braking effectiveness of a friction material at elevated temperature, typically in the range of 300–400 °C [8]. It has been reported that the fade behavior

Table 4 $\bar{\mu}$ and μ-recovery at different temperature cycles tested at 700 rpm

Temperature (temperature cycle)	Material				
	RM	CAR 7.5%	CAR 15%	CELL 7.5%	CELL 15%
100 °C (100–350–100 °C)					
$\bar{\mu}$	0.26	0.30	0.28	0.35	0.38
μ-Recovery (%)	97	115	115	94	95
150 °C (150–350–150 °C)					
$\bar{\mu}$	0.25	0.29	0.25	0.33	0.34
μ-Recovery (%)	102	117	115	108	107
200 °C (200–350–200 °C)					
$\bar{\mu}$	0.21	0.25	0.24	0.21	0.3
μ-Recovery (%)	111	120	116	120	138

could be dominated by the decrease in the mechanical strength, thermal degradation of organic matrix and the formation of load-carrying friction film causing an effective increase in the real contact area and consequently reduction in applied pressure on the friction material [42–44]. However, due to lower thermal stability of rubber material compared with thermosetting resin [45, 46], thermal degradation for RBFM is expected to be more prominent.

In this investigation, the fade behavior is evaluated by the variation of COF with temperature during the thermal stage of friction test where a continuous braking is applied during which the drum temperature allows for increasing by the use of the electric heater and the friction-induced heat. Figure 3 illustrates the variation of COF with temperature at various drum velocities during the thermal stage. In most cases a reduction in COF with temperature is observed. Moreover, it is also inferred that the thermal stage of friction test ends up at different drum temperatures showing the maximum temperature attainable at the end of thermal stage for each composite friction material (see T_{max} values in Table 5). As the continuous braking along with the same heating up program was applied during the thermal stage, the maximum temperature is thought to be due to the friction-induced heat during the braking and the thermo-physical properties of the specimens. In all cases, the drum temperature (T_{max}) increases by the increase of sliding velocity because of higher frictional heat generation [22]; however, the T_{max} is always the lowest for the CAR composites among other specimens. This can possibly be attributed to low COF, leading to low frictional heat [22], high thermal conductivity as well as the endothermic formation of oxygen complexes on the surface of carbon fibers [15]. On the other hand, CEL composites indicate highest drum temperature because of its high COF and exothermic degradation of cellulose fiber [15, 36].

According to Fig. 3, it is revealed that the variation of COF with temperature is dependent upon the sliding velocity. In the other word, the extent of COF loss at high sliding velocity for all composites is found to be lower than that of low sliding velocity. As discussed in our previous study [22], rubber-to-glass transition of rubber component, which is appeared mostly at higher sliding velocities, can be responsible for such behavior. As the rubber constituent forms the dominant portion of the composite, such behavior is much probable. As stated in Table 5, the μ-fade for RM shows a remarkable improvement above 300 rpm which can be explained by the significant change of the composite properties caused by the rubber-to-glass transition phenomenon.

Low μ-fade values presented in Table 5 and small variation of COF with temperature illustrated in Fig. 3b, c demonstrate critical role of carbon fiber in improving the fade behavior of RBFMs. This behavior can be described by the higher thermal conductivity and superior thermal stability of carbon fiber. In addition, lower drum temperature achievable for CAR composites, as mentioned above, can protect the composite from the excessive thermal degradation leading to the great improvement in the fade behavior. In this type of fiber added composites, similarly with RM, the COF-T curve at the drum speed of 300 rpm differs from that of 500 and 700 rpm. This suggests that the presence of carbon fiber in the friction material does not influence rubber-to-glass transition behavior mentioned above for fiber free RBFM.

The variation of COF with temperature for CEL composites is shown in Fig. 3d, e and the corresponding μ-fade values are presented in Table 5. It is found that CEL composites exhibit the greatest values of μ-fade, indicating very poor fade behavior of cellulose fiber. This can be attributed to low degradation temperature of the cellulose fiber. The degradation of cellulose fiber at low temperatures may lead to the formation of thermal voids in the composite which can destroy the integrity of the system severely [15, 36]. For CEL 15%, because of higher volume fraction of thermal degradable cellulose fiber, the reduction of COF with temperature is much more pronounced so that a tremendous loss in COF is observed around 200 °C for

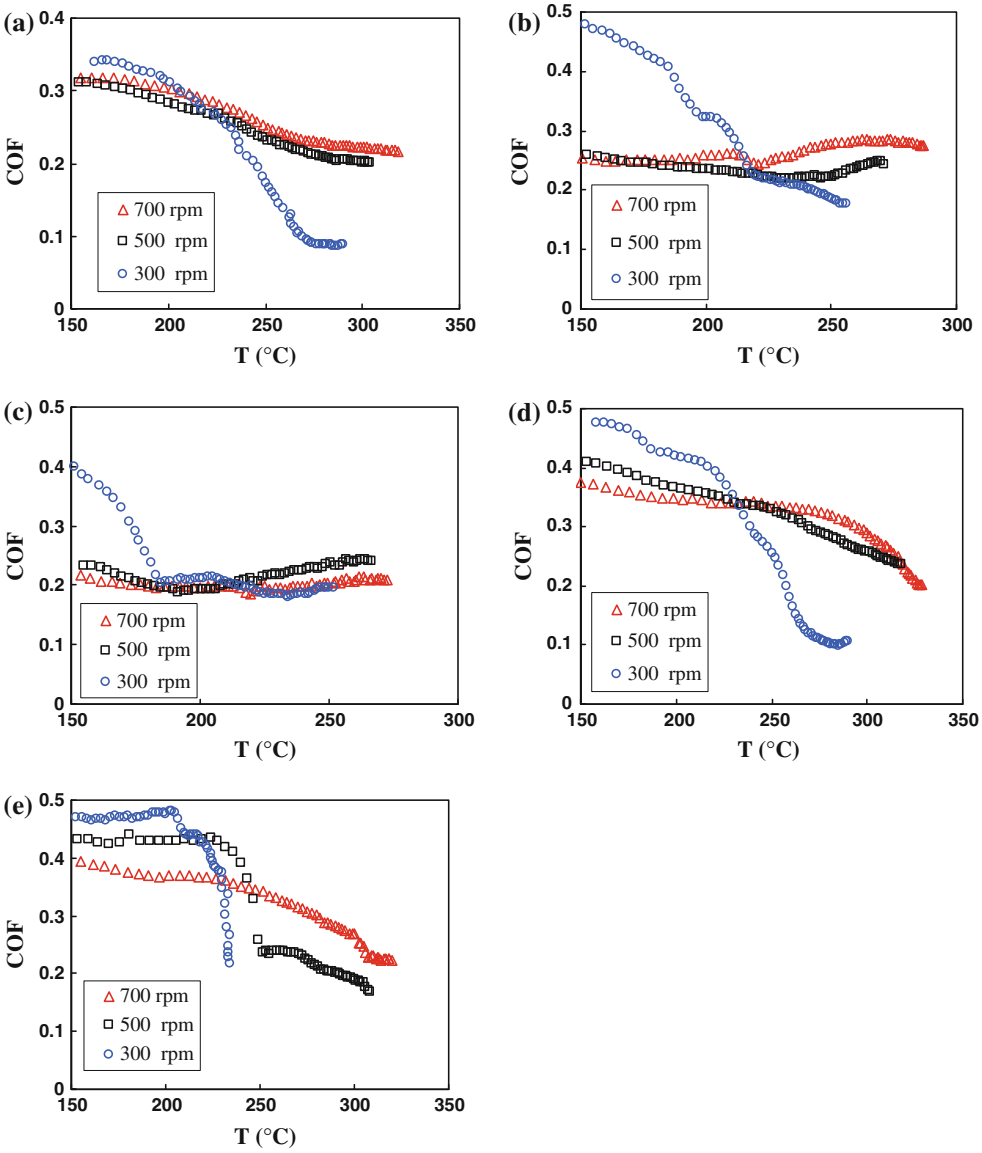

Fig. 3 Variations of COF with temperature during thermal stage at different sliding velocities for **a** RM, **b** CAR 7.5%, **c** CAR 15%, **d** CEL 7.5%, and **e** CEL 15%

Table 5 Thermal and fade behaviors of the samples

Properties at different sliding velocities (rpm)	Material				
	RM	CAR 7.5%	CAR 15%	CELL 7.5%	CELL 15%
300 rpm					
μ-Fade (%)	59.3	24.7	22	65.6	41.9
T^{a}_{max} (K)	563	529	528	563	506
500 rpm					
μ-Fade (%)	17.4	15.6	21.6	26.8	46.9
T^{a}_{max} (K)	577	544	540	591	581
700 rpm					
μ-Fade (%)	15.9	17	20.3	37.9	31.6
T^{a}_{max} (K)	591	560	546	602	593

[a] T_{max}: maximum temperature of disc during the thermal stage

drum speed of 300 rpm (see Fig. 3e). In this case, the influence of sliding speed on COF–*T* curves is also obvious which can be explained by the phenomenon of the glass-to-rubber transition; although this transition shifts to higher sliding velocity, i.e., 700 rpm, at high cellulose fiber content (see Fig. 3e).

Figure 4 shows the variations of COF with temperature during thermal stage at various temperature cycles but with specified sliding velocity of 700 rpm where all samples show glassy behavior. As it is evident, RM and CAR composites reveal almost similar COF–*T* curves (Fig. 4a–c) at various temperature cycles. This suggests that the fade behavior is not influenced by the previous temperature history in these compounds. However, CEL friction materials exhibit a reduction in COF at the temperature cycles with higher values. As the cellulose fiber is

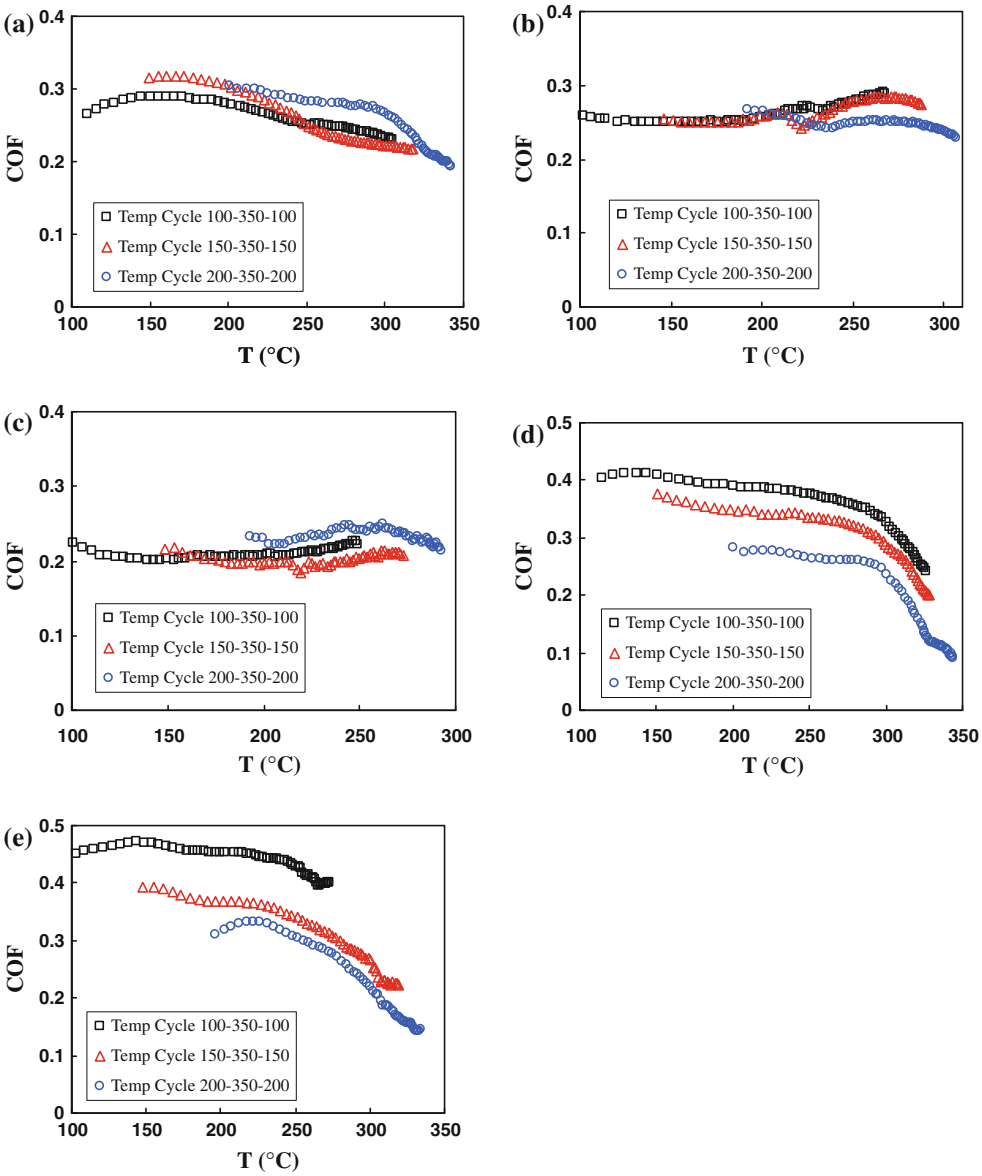

Fig. 4 Variations of COF with temperature during thermal stage at various temperature cycles processed at 700 rpm for **a** RM, **b** CAR 7.5%, **c** CAR 15%, **d** CEL 7.5%, and **e** CEL 15%

thermally degraded at relatively low temperature, i.e., 140 °C onward [15, 33, 36, 37]; therefore the observed behavior is expected. As a matter of fact, degradation of cellulose fibers possibly in the preliminary stage results in weaker load bearing capacity of the composite and consequently lower COF.

SEM analysis and wear characteristics

Figure 5 shows the specific wear rate of employed RBFMs against sliding velocities and the drum temperature. In addition, the SEM microphotographs of the surface of composites worn at two different sliding velocities are displayed in Figs. 6, 7, and 8. According to Fig. 5, RM indicates low specific wear rate at 500 and 700 rpm while higher wear rate is observed at 300 rpm. Higher wear rate of RM at 300 rpm can be associated to the lower mechanical properties of the composite due to the rubbery state of the matrix at this sliding velocity while at higher sliding velocities the mechanical properties are enhanced by transition of rubbery state to the glassy behavior [22]. Presence of big crack on the worn surface of RM examined at 300 rpm (Fig. 6b) can be related to such weak mechanical properties at this sliding condition. Wear thinned and overlapped patches are detected on the worn surface of RM at 700 rpm as shown in Fig. 6a. The presence of these multilayer secondary plateaus contributes to wear resistance of RM composite. High roughness of worn surface of RM composite at 700 rpm (see Table 2) also confirms the presence of uneven multilayer secondary plateaus.

CAR 7.5% demonstrates low and almost unvarying specific wear rate with sliding velocity (Fig. 5a). A fiber

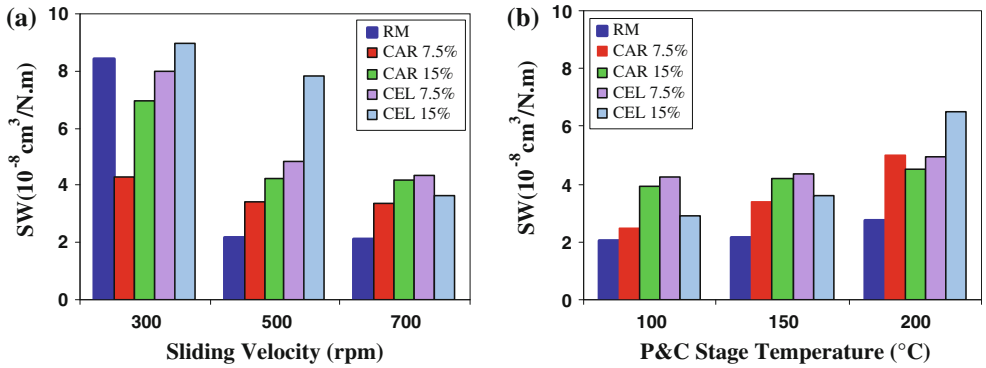

Fig. 5 Specific wear rate of friction materials versus **a** sliding velocity processed at temperature cycle of 150–350–150 °C, **b** drum temperature done at 700 rpm

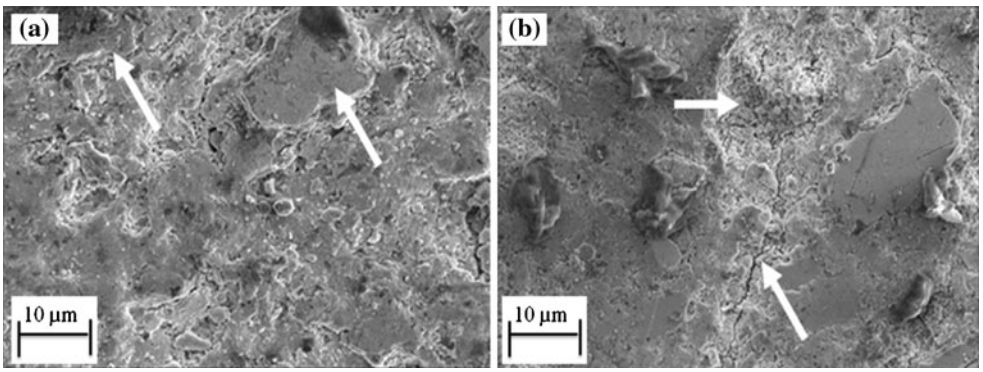

Fig. 6 Worn surface of RM at sliding velocity of **a** 700 rpm, **b** 300 rpm processed at temperature cycle of 150–350–150 °C

that is non-abrading to the counterface such as carbon fiber can promote the formation of a tenacious and thin transfer film on the counterface that can help in reducing the wear rate of composite after a short running-in period [1]. Additionally, high thermal conductivity of carbon fiber, high real contact area and endothermic formation of surface oxygen complexes on the surface of carbon fiber [47] are significant parameters in controlling temperature increase which leads to maintaining friction material integrity at high temperatures. The resultant of all these factors is high wear resistance of CAR 7.5%.

From Fig. 7, the presence of carbon fiber is clearly evidenced on the worn surface of carbon fiber-filled composites. In addition, partially coverage of surface of carbon fiber by the matrix suggests the existence of some interaction between the carbon fiber and the matrix. In the micrograph corresponding to CAR 7.5% (Fig. 7a), the following stages of wear mechanism can be recognized: (a) matrix wear and fiber thinning, (b) fiber breakage, (c) interfacial debonding, and (d) removal of fiber fragments. The latter stage is often induced by the asperities of counterface which leave open longitudinal cavities on the worn friction surface [34]. Worn surface morphology of CAR 15% at 700 and 300 rpm is depicted in Fig. 7c, d, respectively. Similar mechanisms as CAR 7.5% can be conceived for CAR 15%. Nevertheless larger volume fraction of carbon fiber, as lubricating agent and thermally conductive and thermally stable ingredient, leads to some dissimilarity in wear mechanisms undoubtedly.

Figure 8 shows the worn surface morphology of CEL composites. As deduced from the micrographs, there is no evidence about the presence of cellulose fiber on the worn surface. A possible explanation is that the cellulose fiber is degraded at the contact surface, followed by filling of the cavity by means of the abraded materials and degraded constituents. As it is seen in Fig. 8a, the friction surface is covered by secondary plateaus chiefly. Low roughness of CEL composites at 700 rpm (Table 2) can be due to the presence of smooth and coherent secondary plateaus. Figure 8b exhibits the worn surface of CEL composites at 300 rpm. Slight wear tracks by third body abrasion, detachment of secondary plateaus and cavities wherefrom ingredients were lost, are the clear characteristics of worn surface in this case.

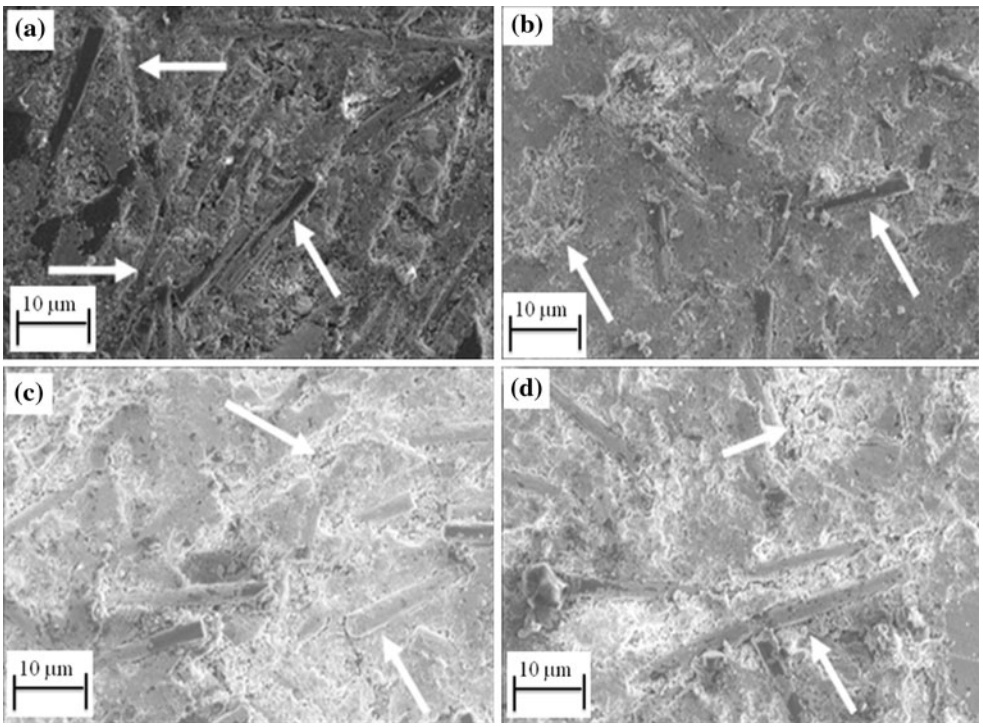

Fig. 7 Worn surface of carbon fiber added friction materials processed at temperature cycle of 150–350–150 °C. **a** CAR 7.5% at 700 rpm, **b** CAR 7.5% at 300 rpm, **c** CAR 15% at 700 rpm, and **d** CAR 15% at 300 rpm

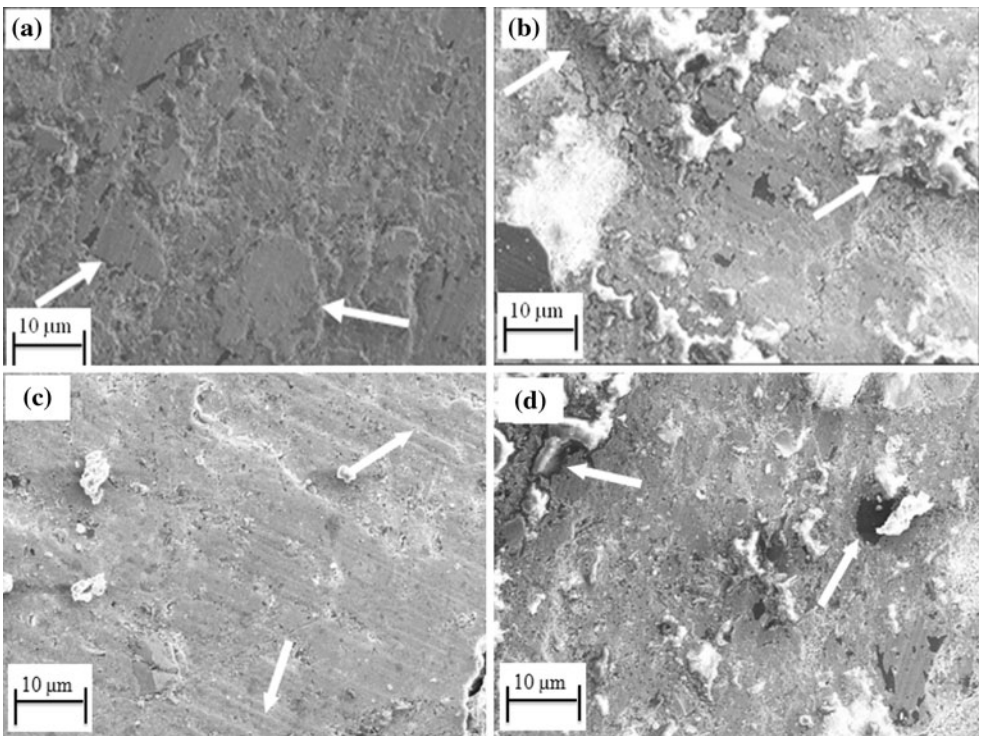

Fig. 8 Worn surface of cellulose fiber added friction materials processed at temperature cycle of 150–350–150 °C. **a** CEL 7.5% at 700 rpm, **b** CEL 7.5% at 300 rpm, **c** CEL 15% at 700 rpm, and **d** CEL 15% at 300 rpm

It is realized that incorporation of cellulose fiber increases the wear rate (see Fig. 5a), while the cellulose fiber-filled composites shows a relative low specific wear rate at 700 rpm. The higher wear rate at low sliding velocities, i.e., 300 and 500 rpm, can be attributed to the thermal degradation of cellulose fiber. In general, thermal degradation of cellulose fiber due to breakage of weak β-glycoside linkage leads to the formation of voids which act like cracks intensifying the further propagation of already existing flaws [15, 36]. On the other hand, this thermal degradation is energetically exothermic that results in higher temperature in the friction surface which can heighten the wear process [15, 28]. In addition to thermal degradation, presence of abrasive wear debris, rubbery state of the friction composite and low strength of friction and transfer layers may be responsible for low wear resistance of CEL composites. The low wear rate of CEL composites at 700 rpm can be attributed to the formation of protective secondary plateaus (Fig. 8) along with the glassy behavior of composite due to strong viscoelastic response [22].

Figure 5b demonstrates the variations of specific wear rate with drum temperature at sliding velocity of 700 rpm. Note that this temperature denotes the drum temperature at preliminary and complementary stages of friction tests. It is found that the influence of temperature is not as much as the sliding velocity. This indicates that the wear rate is not influenced by the drum temperature at preliminary and complementary stages and it is thought to be dominated by the harsh conditions experienced at thermal stage which was the same for all specimens.

Conclusions

The experimental investigation on the tribological behavior of RBFMs filled with carbon fiber and cellulose fiber was performed. It was observed that the maximum attainable drum temperature caused by the friction-induced heat for the CAR composites is lower than that of the CEL and fiber free composites. Carbon fiber influences COF slightly due to the lubricating role of this material as well. However, it enhances the wear resistance and improves greatly the μ-fade and μ-recovery of RBFMs due to its superior thermal characteristics. CEL composites show weak fade behavior and low wear resistance particularly at low sliding velocities due to its low thermal stabilities. Despite thermal degradation of cellulose fibers, the corresponding composites indicate high COF and good recovery behavior because of the presence of abrasive wear debris in the friction interface. Rubber-to-glass transition which was reported in our previous work was also observed for highly loaded fiber systems, even though a shift in the transition sliding velocity is recognized for CEL 15% composite.

Acknowledgement The authors are grateful for financial support of the Railway Research Center of Iran in this research work.

References

1. Friedrich K, Schlarb AK (2008) In: Briscoe BJ, Sinha SK (eds) Tribological applications of polymers and their composites: past, present and future prospects. Engineering series, vol 55. Elsevier, Amsterdam
2. Kim SJ, Jang H (2000) Tribol Int 33:477
3. Yi G, Yan F (2007) Wear 262:121
4. Bijwe J (1997) Polym Compos 18:378
5. Gopal P, Dharani LR, Blum FD (1994) Wear 174:119
6. Rhee SK, Jacko MG, Tsang PHS (1991) Wear 146:89
7. Adelmann JC (1976) US Patent 3959194
8. Littlefield JB (1982) US Patent 4313869
9. Abbasi F, Shojaei A, Katbab A (2001) J Appl Polym Sci 81:363
10. Gibson PA (1996) In: IMechE seminar publication in railway traction and braking, pp 75–85
11. Ludema KC (1996) Friction, wear, lubrication, 1st edn. CRC Press Inc, Boca Raton
12. Bijwe J, Nidhi MN, Satapathy BK (2005) Wear 259:1068
13. Dureja N, Bijwe J, Gurunath PV (2009) J Reinf Plast Compos 28(4):489
14. Ho SC, Chern Lin JH, Ju CP (2005) Wear 258:861
15. Satapathy BK, Bijwe J (2004) Wear 257:573
16. Chang HW (1983) Wear 85:81
17. Giltrow JP, Lancaster JK (1970) Wear 16:359
18. Bijwe J, Tewari US (1989) Wear 132:247
19. Gopal P, Dharani LR, Blum FD (1995) Wear 181–183:913
20. Shojaei A, Fahimian M, Derakhshandeh B (2007) Compos Sci Technol 67:2665
21. Haddadi E, Abbasi F, Shojaei A (2005) J Appl Polym Sci 95:1181
22. Saffar A, Shojaei A, Arjmand M (2010) Wear 269:145
23. Lancaster JK (1968) J Phys D 1:549
24. Gopal P, Dharani LR, Blum FD (1996) Wear 193:199
25. Male J (1984) Diesel Engine Supt 62:47
26. Qu X, Zxang L, Ding H, Liu G (2004) Polym Compos 25(1):94
27. Astrom BT (1997) Manufacturing of polymer composites, 1st edn. Chapman & Hall, London
28. Agarwal BD, Broutman LJ (1990) Analysis and performance of fiber composite. Wiley, New York
29. Satapathy BK, Bijwe J (2006) Composites A 37:1557
30. Nicholson G (1995) Facts about Friction. P & W Price Enterprise Inc., Gedoran America Limited, Winchester
31. Griffith AM (1980) US Patent 4217255
32. UIC code 541-4 OR (1990) Brakes with composition brake blocks, 2nd edn. International Union of Railways
33. Steinmann HW (1985) In: Lewin M, Pearce EM (eds) Proceedings of international fiber science and technology, vol 4, series 7. Marcel Dekker, New York, pp 1001–1078
34. Friedrich K, Schlarb AK (2008) In: Chang L, Zhang Z, Ye L, Friedrich K (eds) Synergistic effects of nano particles and traditional tribo-fillers on sliding wear of polymeric hybrid composites. Engineering series, vol 55. Elsevier, Amsterdam, pp 35–58
35. Friedrich K, Schlarb AK (2008) In: Bahadur S, Shwartz CJ (eds) The influence of nanoparticle fillers in polymer matrices on the

formation and stability of transfer film during wear. Engineering series, vol 55. Elsevier, Amsterdam, pp 17–33
36. Ott M, Spvrling HM, Grafflin MW (1954) Chemical nature of cellulose and its derivatives in cellulose and cellulose derivative. Part I. Interscience, New York, pp 140–167
37. Satapathy BK, Bijwe J (2005) J Reinf Plast Compos 24(6):579
38. Dwyer-Joyce RS, Sayles RS, Ioannides E (1994) Wear 175:133
39. Stachowiak GB, Stachowiak GW (2001) Wear 249:201
40. Wang M, Kang Q, Pan N (2008) J Appl Therm Eng 29:418
41. Li H, Jacob KI, Wong CP (2003) IEEE Trans Adv Packag 26:25
42. Herring JM (2005) SAE Trans 670146:558
43. Anderson AE (1990) In: ASM hand book, vol 18. ASM Materials Information Society, Metals Park, pp 569–577
44. Wirth A, Eggleston D, Whitaker R (1994) Wear 179:75
45. Shojaei A, Faghihi M (2010) Polym Adv Technol 21:356
46. Derakhshandeh B, Shojaei A, Faghihi M (2008) J Appl Polym Sci 108:3808
47. Blanco C, Bermejo J, Marsh H, Mendenez R (1997) Wear 213:1